Materials Science in Semiconductor Processing 15 (2012) 461–466

Contents lists available at SciVerse ScienceDirect

Materials Science in Semiconductor Processing

journal homepage: www.elsevier.com/locate/mssp

Review

Evaluation of the hydrostatic pressure effect on Mn/p-Si Schottky barrier diode electrical parameters and interface states

Songül Fiat [a,*], Güven Çankaya [b]

[a] Gaziosmanpaşa University, Faculty of Arts and Science, Department of Physics, 60240 Tokat, Turkey
[b] Yıldırım Beyazıt University, Faculty of Engineering and Natural Sciences, Materials Engineering, 06030 Ankara, Turkey

ARTICLE INFO

Available online 24 April 2012

Keywords:
Si
Schottky barrier diodes
Electrical characterization
Interface states

ABSTRACT

Mn/p-Si Schottky barrier diode (SBD) electrical parameters and interface state density have been investigated with current–voltage (*I–V*) characteristics and Cheung's functions employing hydrostatic pressure. The interface state density of the diodes has an exponential growth with bias from the midgap towards the top of the valance band. We have seen that the Schottky barrier height (SBH) for Mn/p-Si SBD has a pressure coefficient of 1.61 meV/kbar (16.1 meV/GPa). We have reported that the p-type barrier height exhibited a weak pressure dependence, accepting that the Fermi level at the interface do not shift as a function of the pressure.

Contents

1. Introduction

Schottky barrier diodes (SBDs) are the basis of a number of semiconductor electronic devices, including microwave diodes, field-effect transistors (FETs), solar cells and photodetectors. Schottky contacts are rectifying metal–semiconductor (MS) junctions and their forward current consists of majority carriers injected from the semiconductor into the metal. Knowledge of the conduction mechanism across a Schottky barrier is essential to calculate Schottky barrier parameters and explain the observed effects and behaviors [1].

We chose silicon (Si) as a semiconductor material due to its lower cost and the availability of well established processing technology. It has an indirect band gap and is still widely used as the material of choice for the fabrication of photo-devices in Si-based integrated optoelectronic circuits (OEICs) [2]. Si has remained the most popular choice due to its history of reliable performance. Schottky barrier height (SBH) on p-type Si is usually in the range 0.4–0.7 eV independent of the metallization [3,4]. In addition, deviations of the current–voltage (*I–V*) characteristics can be explained successfully by means of these device parameters such as the ideality factor, the series resistance and the SBH. One of the most interesting properties of a metal–

* Corresponding author. Tel.: +90 0356 252 16 16; fax: +90 0356 252 15 85.
E-mail address: songulfiat@yahoo.com (S. Fiat).

1369-8001/$ - see front matter © 2012 Elsevier Ltd. All rights reserved.
http://dx.doi.org/10.1016/j.mssp.2012.03.004

semiconductor interface is its Schottky barrier height, which is a measure of the mismatch of the energy levels for majority carriers across the metal–semiconductor interface. The SBH controls the electron transport across the metal–semiconductor interface and is of vital importance to the successful operation of any semiconductor device [5,6]. The phenomenon of Schottky contact formation at MS interfaces has been studied actively for over three decades.

Many researchers have explored various metal schemes for the fabrication of Schottky contacts on p-type Si; e.g., H-terminated Zn [7], Sn/Rhodamine-101 [8], Ta [9], PtSi [10], Cr [11], Cu [12], Cu_2O [13], In [14], Pb [15], Zn and Sn [16]. Ucar et al. [17] investigated the hydrostatic pressure effect on Al/conducting polymer (P3DMTPT)/p-Si/Al. They applied pressure (0.00–6.00 kbar) to this structure and the SBH increased from 0.63 eV to 0.72 eV with increases in the hydrostatic pressure whereas the ideality factor decreased.

Liu et al. [18] applied hydrostatic pressure on the SBH of Ga-polarity n-$Al_{0.08}Ga_{0.92}N$. The SBH increased by 8.9 mV/kbar. They observed an increase in SBH with increasing pressure and attributed this to a combination of band structure and piezoelectric effects. Also, Ahlskog et al. [19] prepared a poly(3-alkylthiophene) field effect transistor and a Schottky diode to observe the hydrostatic pressure effect. Gworek et al. [20] studied the pressure dependence of the Cu, Ag, and Fe/n-GaAs (110) on SBH.

In this study, we investigated the hydrostatic pressure dependence of the electrical characteristic parameters and interface state density by using the thermionic emission (TE) theory, and Cheung's functions in the pressure range of 0.00–7.00 kbar. Analysis of the *I–V* characteristics of SBDs based on the TE theory usually reveals an ordinary increase in the SBH and a decrease in the ideality factor with an increase in hydrostatic pressure. Furthermore, the forward bias *I–V* characteristics were linear in the semi-logarithmic scale at low voltages but deviated considerably from linearity due to the effect of the parameters, such as the series resistance, the interfacial layer and the interface states when the applied voltage was sufficiently large [21].

Recently, hydrostatic pressure as well as the temperature dependence of SBDs has been investigated in order to study the optical and electrical properties and the Schottky barrier formation. It is well known that these properties are sensitive to the application of external pressure and to the variations in temperature as well as non-idealities such as the interface state, interface oxide layer, interface fixed charges, interface traps and series resistance [22–24]. So, in the recent years, hydrostatic pressure has been used as a tool for studying the optical and electronic properties of semiconductors and SBDs. The experimental evidence shows that pressure or stress plays a very important role in the transport properties in semiconductor materials [25]. The well-known effects are the energy band gap variation with hydrostatic pressure, the stress-induced piezoelectric field in III–V compound semiconductors, and the change of the band edge curvature and the band edge splitting with uniaxial pressure [26].

Control of the barrier height is critical for the successful operation of devices based on the Schottky contacts. Unstable contacts result in barrier height changes, increased leakage current, and other undesirable effects that degrade the electrical performance of the device. However, despite years of extensive research and widespread use of the Schottky contacts in device technology, the fundamental mechanism responsible for the formation of the Schottky barrier is still a research area. This work focuses on experimental measurements of the pressure coefficient of the Schottky barrier height to help elucidate the mechanism of the Fermi level pinning in Mn/p-Si contacts. In this connection, it has been shown that Φ_b shows a 0.001 eV (1 meV) decrease with increasing hydrostatic pressure.

2. Experiment details

The samples were prepared using mirror cleaned and polished p-type Si (B doped to about $10^{15}\,cm^{-3}$) wafers with (100) orientation, 5–10 Ω cm resistivity and 400 μm thickness. The p-type Si wafers with low resistivity Ohmic back contacts were then subjected to the evaporation of Al followed by a temperature treatment at 575 °C for 3 min. Each wafer was cut into pieces of 5 mm × 5 mm. These were chemically etched using HF/H_2O for 30 s to remove detritus such as native oxide from the front surface of the samples. The Schottky contacts were formed by evaporating Mn as dots with a diameter of about 1 mm onto the mirror surfaces (diode area $=7.85\times10^{-3}\,cm^2$). Thickness of the Mn film was ~900 Å. All evaporation processes were performed in a vacuum coating unit at about 10^{-5} mbar. Thus, the Mn/p-Si samples were obtained. The pressure cell consisted of a conventional piston cylinder system constructed of AISI 4340 steel. Special transformer oil was used to transmit the pressure. Pressure in the cell was measured by observing change in the resistance of a manganin wire. The Mn/p-Si Schottky diodes were located in the pressure cell with a special designed sample holder and *I–V* measurements under 0.00–7.00 kbar hydrostatic pressure were made by the electrical connections from the cell to the measuring device and the *I–V* characteristic of diodes were measured and plotted.

3. Results and discussion

For a Schottky barrier diode, current transport is due to majority carriers and it is described by the TE theory over the interface barrier [27]. The thermionic emission current voltage expression is mentioned as

$$I=I_0\exp\left(\frac{q(V-IR_s)}{nkT}\right)\left[1-\exp\left(-\frac{q(V-IR_s)}{kT}\right)\right] \tag{1}$$

where I_0 is the saturation current derived from the straight line intercept of $\ln I$ at $V=0$ and is expressed as

$$I_0=AA^*T^2\exp\left(-\frac{q\Phi_b}{kT}\right) \tag{2}$$

where q is the electron charge, V is the applied voltage, A is the effective diode area, k is the Boltzmann constant, T is the absolute temperature, and A^* is the effective Richardson constant of $32\,A\,cm^{-2}\,K^{-2}$ for p-Si [28]. I_0 values were found as 3.52×10^{-7} A at 0.00 kbar and 2.28×10^{-7} A at 7.00 kbar (Fig. 1). When a metal and a semiconductor are brought into contact, a potential

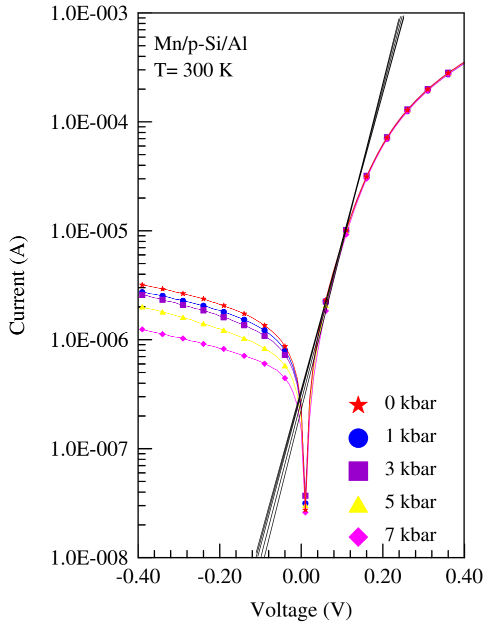

Fig. 1. Experimental forward and reverse bias current versus voltage (I–V) characteristics of the Mn/p-Si Schottky barrier diode with different pressure values (the black lines belong to fit lines of each curve).

barrier occurs at the interface which is found to exhibit rectifying properties. Φ_b is the SBH, defined as the difference between the edge of the respective majority carrier band of the semiconductor and the Fermi level at the interface.

The variation in SBH with pressure was fitted with the equation

$$e\Phi_b(P) = e\Phi_b(0) + \alpha P \tag{3}$$

with a pressure coefficient $\alpha = 1.61$ meV/kbar obtained from the I–V curve (16.10 meV/GPa) (Fig. 2). Thus, the pressure coefficient of $d\ \Phi_b(P)/dP = 1.61$ meV/kbar for the barrier height of our own Mn/p-Si device shows that the Fermi level at the Mn/p-Si interface is pinned relative to the valance band maximum as a function of the pressure as indicated in the MIGSs model [29–31]. This slight increase in the barrier height with increasing pressure should be related to the increase in the band gap. We observed that, in an n-type structure, SBH can be changed with increasing pressure [31–33], while in a p-type the SBH change is limited and exhibits a weak pressure dependence [17,30] as shown in Fig. 4.

van Schilfgaarde et al. [34] have reported theoretically that the pressure coefficient of the SBH is different for metal/semiconductor interfaces with and without defects. Phatak et al. [35] successfully explained the pressure-induced changes in the Fermi level pinning by defect mediated models in a Au/n-GaAs diode. Werner [36] and Werner and Güttler [37] concluded that the temperature or pressure coefficients of the SBH depend on the chemical nature of the contact metal and a strong influence of interface crystallography.

In addition, the ideality factor, n presents how closely the diode follows the ideal diode equation and can be

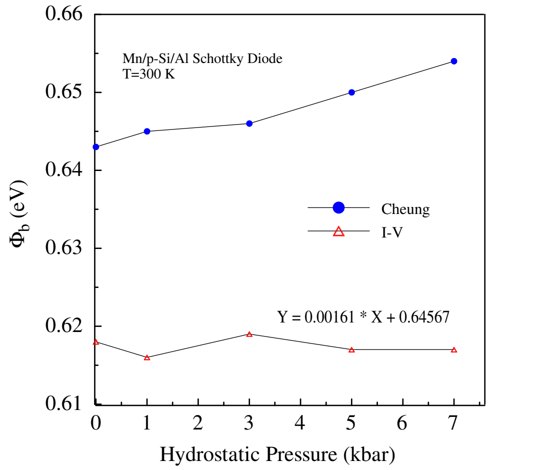

Fig. 2. Barrier height versus pressure plots for the Mn/p-Si Schottky barrier diodes according to I–V characteristics and Cheung's functions.

determined from the slope of the linear portion of $\ln(I/(1-\exp(-qV/kT))$ versus. V plot. The ideality factor can be written as

$$n = \frac{q}{kT}\left[\frac{dV}{d(\ln I)}\right] \tag{4}$$

The ideality factors of the Mn/p-Si Schottky diode have been calculated as 1.23 at 0.00 kbar and 1.12 at 7.00 kbar, respectively ($n > 1$) (Table 1). n equals to one for an ideal diode. However, n has usually a value greater than unity. Higher values of n can be attributed to the presence of the interfacial thin native oxide layer and a wide distribution of low-SBH patches (or barrier inhomogeneities), and to the bias voltage dependence of the SBH [27].

The values of n show that the devices obey the MIS configuration rather than the ideal Schottky diode. The interface oxide layer may form either during surface preparation and metal evaporation or during postdeposition thermal annealing [27,38]. If the Si surface is prepared by the usual polishing and chemical etching, and the evaporation of metal is carried out in a conventional vacuum system having a pressure of around 10–5 mbar, the Si surface is inevitably covered with a thin insulating film. This oxide layer is between 5 and 10 Å thick, depending on the method of surface preparation. For a sufficiently thick interface layer, the interface states are in equilibrium with the semiconductor and cannot interact with the metal [27,39,40]. Furthermore, at high currents there is always a deviation of the ideality, which has been clearly shown to depend on the interface state density and bulk series resistance, associated with bulk material Si and the ohmic back contact, when the applied voltage is sufficiently large as one would expect [41].

The image force effect, generation–recombination of electron–hole couples, and the tunneling effect may be the other reasons for the high values of n [42–44].

Furthermore, it was seen that the forward bias $\ln I$ versus V curve are not exactly linear. Therefore, the Φ_b and n values of the I–V curve must be determined by the

Table 1
Electrical parameters of the Mn/p-Si/Al Schottky diodes obtained from I–V characteristics at different pressure values.

Pressure (kbar)	n (I–V)	n (Cheung)	Φ_b (eV) (Cheung)	R_s (Ω) $[(dV/d\ln I)-I]$	R_s (Ω) $[H(I)-I]$
0.00	1.23	1.64	0.618	395.58	403.51
1.00	1.22	1.68	0.616	403.08	409.41
3.00	1.19	1.67	0.619	390.02	390.92
5.00	1.15	1.68	0.617	392.39	390.89
7.00	1.12	1.74	0.617	386.69	384.72

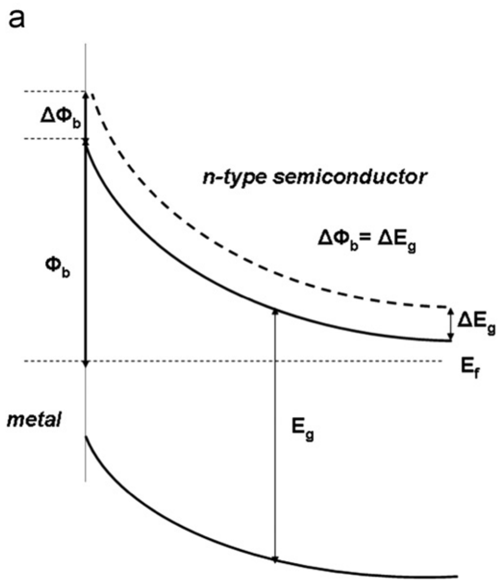

Fig. 3. Band structure of metal/semiconductor structures under hydrostatic pressure: (a) for Metal/n-type semiconductors and (b) for Metal/p-type semiconductors.

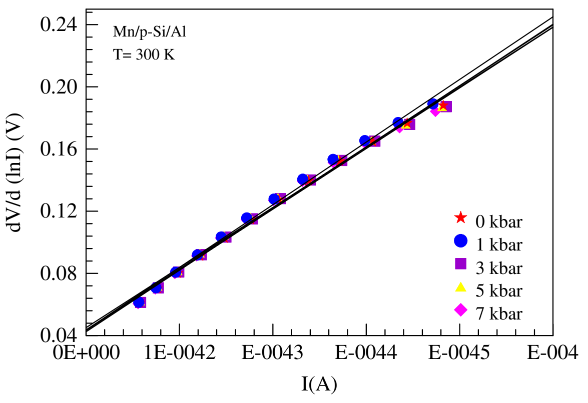

Fig. 4. $dV/(\ln I)$ versus I plots for the Mn/p-Si Schottky barrier diode with different pressure values.

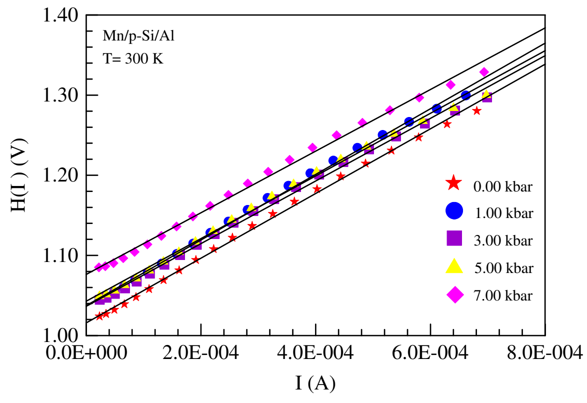

Fig. 5. $H(I)$ versus I plots for the Mn/p-Si Schottky barrier diode with different pressure values.

analysis of Cheung and Cheung [45]. The lower the interface density and the series resistance, the greater is the range over which ln$I$–V does in fact yield a straight line. According to Cheung and Cheung [45], the forward biased I–V characteristics for a large applied voltage ($V > 3kT/q$) from the TE model of a Schottky diode with series resistance can be expressed as Eq. (1). The IR_s term indicates the voltage drop across the series resistance of the diode described in the equation. The values of the series resistance R_s can be determined from the following equations (Fig. 3):

$$\frac{dV}{d(\ln I)} = IR_s + n\frac{kT}{q} \tag{5}$$

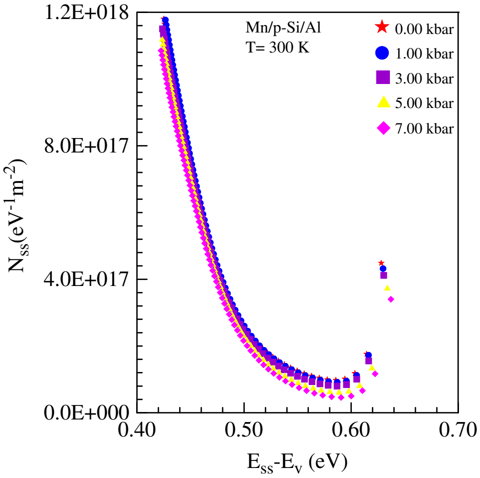

Fig. 6. Density of interface states of the Mn/p-Si Schottky barrier diode as a function of $E_{SS}-E_V$ obtained from *I–V* characteristics at different hydrostatic pressures.

and

$$H(I) = V - \left(\frac{nkT}{q}\right)\ln\left(\frac{I}{AA^{*}T^{2}}\right), \tag{6}$$

where $H(I)$ is given by (Fig. 5)

$$H(I) = IR_s + n\Phi_b \tag{7}$$

where Φ_b is the real barrier height extracted from the lower voltage part of forward *I–V* characteristics. The $dV/d(\ln I)$ plot is a straight line region which dominates the series resistance. In the plot of $dV/d(\ln I)$ versus *I*, its slope gives the series resistance while its intercept with the *y*-axis gives the ideality factor. The ideality factor, *n*, is extracted from the $dV/d(\ln I)$ plot within voltage range where influence of series resistance is significant. Using so obtained value of ideality factor, *n*, the SBH is estimated from plot of a function $H(I)$ given in Eq. (6). It is approximately the straight line which intercepts the *y*-axis at the point equal to $n\ \Phi_b$. The slope of the line provides another way of calculating the series resistance in Eq. (7) which in our case turned out to be close to the value obtained from Eq. (5).

R_s is in the order of the bulk resistivity, but when $n>1$, the series resistance takes values several magnitude order of resistivity. This R_s is the sum of the neutral bulk and ohmic contact resistance [46,47]. So, the total resistance of the substrate and the contact resistance R_0, must be greater than the substrate resistance where the resistivity of 5–10 Ω cm was assumed for the present p-Si. Therefore, the R_0 values greater than substrate resistance represent approximately the contact resistance at the p-Si/metal interface.

When the interfacial layer is sufficiently thick and the transmission probability between the metal and the interface states is very small, the barrier height shift can be expressed as

$$\Delta\Phi_e = \Phi_e - \Phi_{b,0} = (1-c_2)(V-IR_s), \tag{8}$$

with forward bias where

$$c_2 = \frac{1}{n} = \frac{1}{1+\alpha} = \frac{\varepsilon_i}{\varepsilon_i + q^2 N_{ss}\delta}, \tag{9}$$

is a parameter inverse of the well-known ideality factor *n* and is a measure of conformity of the diode to pure thermionic emission.ε_i is the permittivity of the interfacial layer. δ is the thickness of the interfacial layer in which holes move through tunnel. The Φ_e is assumed to be bias dependent owing to the presence of an interfacial layer and interface states located at the interfacial layer-semiconductor interface and N_{ss} is the expression of the density of interface states for metal/semiconductor diodes (Fig. 6). The applied voltage dependence of the barrier height
is obtained as

$$\alpha = \frac{q^2 N_{ss}\delta}{\varepsilon_i}, \tag{10}$$

$$\frac{d\Phi_e}{dV} = \beta = 1 - \frac{1}{n(V)}, \tag{11}$$

where β is the voltage coefficient of the effective height Φ_e used in place of the barrier height Φ_b. In p-type semiconductors, the energy of the interface states E_{ss} with respect to the top of the valance band at the surface of the semiconductor is given by [48]

$$E_{ss} - E_v = q\Phi_e - qV \tag{12}$$

The N_{ss} has an exponential rise with bias from the midgap towards the top of the valance band for each hydrostatic pressure value. The same behavior of N_{ss} with temperature [49–51], ageing time [52], and ray irradiation [53] has also been observed in the Al/p-Si, polypyrrole/p-Si/Al, and Au/n-GaAs diodes. The results of this work show that a metal/semiconductor structure does not exhibit a considerable change in the barrier height and interface state density with increasing pressure, whereas when a different layer is deposited between the metal and semiconductor interface, the diode response changes with pressure so that when the density of interface states is decreased, SBH is seen to increase [8,17].

4. Conclusions

In conclusion, it has been seen that the Mn/p-Si Schottky barrier diode shows the rectifying behavior and the reverse curves exhibit the excellent saturation. Therefore, we can use the simple thermionic emission theory that is for a Schottky type barrier to obtain the characteristic parameters of the device. Thus, it is assumed that the forward bias current of the device is due to thermionic emission current. It is more fully, and accurately, named reverse saturation current which causes diffusion of minority carriers from the neutral to the depletion regions. This current is almost independent of the reverse voltage. Given this, we can say that the major carriers have a strong influence to control the flow in diode.

In this study, we calculated the electrical parameters as a function of hydrostatic pressure that are in close agreement with other studies with regard to the mean values obtained from *I–V* characteristics and Cheung's functions. We have observed that the variation of the SBH (pressure coefficient $\alpha = 1.61$ meV/kbar, (16.10 meV/GPa) for the Mn/p-Si Schottky barrier diode is not due to applied pressure alone. It is also necessary to follow precisely the variation of the semiconductor band-gap because the Fermi level has been accepted as a reference level which is pinned to the valance band maximum at the interface as a function of the pressure. Also, the interface states densities did not show a considerable variation with increasing pressure. The downward concave curvature of the forward bias current–voltage characteristics at sufficiently large voltages is caused by the presence of the effect of series resistance, apart from the interface states, which are in equilibrium with the semiconductor.

Series resistance was determined with the help of the TE theory and Cheung's functions as 395.58–386.69 Ω in $\left[(dV/d\ln I)-I\right]$, 403.51–384.72 Ω in $[H(I)-I]$ at 0.00–7.00 kbar pressure, respectively. However, the improvement in Schottky characteristics for our diode (with ideality factor being close to unity) due to increase in hydrostatic pressure has been usually attributed to removal of the native oxide by the contact material and to stable phases of the interface which are formed by chemical reactions between metal and Si substrate. Therefore it has been found that the Mn/p-Si Schottky barrier height remains reasonably stable up to 7.0 kbar. Likewise, there is a decrease in series resistance with increasing pressure. We have also studied the suitability and possibility of the MS diodes for use in barrier modification with the role of hydrostatic pressure.

References

[1] B. Abay, G. Çankaya, H.S. Güder, H. Efeoğlu, Y.K. Yoğurtçu, Semiconductor Science and Technology 18 (2003) 75–81.
[2] A.D. Stiff, S. Krishna, P. Bhattacharya, S.W. Kennerly, IEEE Transactions on Electron Devices 48 (2001) 1747.
[3] Zs.J. Horvath, M. Adam, I. Szabo, M. Serenyi, V.Vo. Tuyen, Applied Surface Science 190 (2002) 441.
[4] M.O. Aboelfotoh, Solid State Electronics 34 (1991) 51.
[5] V. Janardhanam, A. Ashok Kumar, V. Rajagopal Reddy, P. Narasimha Reddy, Journal of Alloys and Compounds 485 (2009) 467–472.
[6] H. Altuntas, S. Altındal, S. Özçelik, H. Shtrikman, Vacuum 83 (2009) 1060–1065.
[7] Ş. Karataş, A. Türüt, Vacuum 74 (2004) 45–53.
[8] Ş. Karataş, M. Çakar, Synthetic Metals 159 (2009) 347–351.
[9] Y.S. Ocak, M.F. Genisel, T. Kılıçoğlu, Microelectronic Engineering 87 (2010) 2338–2342.
[10] A. Rahman, C.W. Bates Jr., W.P. Lowe, A.F. Marshall, Materials Science and Engineering B 77 (2000) 241–245.
[11] B. Tatar, A.E. Bulgurcuoğlu, P. Gökdemir, P. Aydoğan, D. Yılmazer, O. Özdemir, et al., International Journal of Hydrogen Energy 34 (2009) 5208–5212.
[12] A.A.M. Farag, A. Ashery, E.M.A. Ahmed, M.A. Salem, Journal of Alloys and Compounds 495 (2010) 116–120.
[13] R.K. Gupta, K. Ghosh, P.K. Kahol, Physica E 41 (2009) 876–878.
[14] N. Tuğluoğlu, S. Karadeniz, F. Yakuphanoglu, Physica B 393 (2007) 56–60.
[15] H.A. Çetinkara, A. Türüt, D.M. Zengin, Ş. Erel, Applied Surface Science 207 (2003) 90–199.
[16] Ş. Karataş, Solid State Communications 135 (2005) 500–504.
[17] N. Ucar, A.F. Özdemir, A. Çalik, A. Kokce, Superlattices and Microstructures 49 (2011) 124–131.
[18] Y. Liu, M.Z. Kauser, P.P. Ruden, Z. Hassan, Y.C. Lee, S.S. Ng, et al., Applied Physics Letters 88 (2006) 022109.
[19] M. Ahlskog, J. Paloheimo, H. Stubb, A. Assadi, Synthetic Metals 65 (1994) 77–80.
[20] C.S. Gworek, P. Phatak, B.T. Jonker, E.R. Weber, N. Newman, Physical Review B 64 (2001) 045322.
[21] S. Karadeniz, N. Tuğluoğlu, T. Serin, N. Serin, Applied Surface Science 246 (2005) 30.
[22] G. Çankaya, B. Abay, Semiconductor Science and Technology 21 (2006) 124–130.
[23] M.J. Peanasky, H.G. Drickamer, Applied Physics 56 (1984) 3471–3475.
[24] G. Çankaya, N. Ucar, A. Turut, Physica Status Solidi A 179 (2000) 469–473.
[25] W. Zhang, C. Xue, J. Xiong, B. Xie, T. Wei, Y. Chen, Indian Journal of Pure and Applied Physics 45 (2007) 294–298.
[26] S.C. Jain, M. Wilander, H. Maes, Semiconductor Science and Technology 11 (1996) 641–671.
[27] E.H. Rhoderick, R.H. Williams, Metal–Semiconductor Contacts, Clarendon, Oxford, 1988.
[28] H. Werner, U. Rau, in: J.F. Luy, P. Russer (Eds.), Springer Series in Electronics and Photonics, vol. 32, Springer, Berlin, 1994.
[29] N. Ucar, A.F. Ozdemir, D.A. Aldemir, S. Cakmak, A. Calik, H. Yildiz, et al., Superlattices and Microstructures 47 (2010) 586–591.
[30] M. Çakar, C. Temirci, A. Türüt, G. Çankaya, Physica Scripta 68 (2003) 70–73.
[31] G. Çankaya, N. Uçar, E. Ayyıldız, H. Efeoğlu, A. Türüt, Y.K. Yoğurtçu, Physical Review B 60 (1999) 15944.
[32] W. Shan, M.F. Li, P.Y. Yu, W.L. Hansen, W. Walukiewicz, Applied Physics Letters 53 (1988) 974–976.
[33] S. Aydoğan, Ü. İncekara, A. Türüt, Thin Solid Films 518 (2010) 7156–7160.
[34] M. van Schilfgaarde, E.R. Weber, N. Newman, Physical Review Letters 73 (1994) 581.
[35] P. Phatak, N. Newman, P. Dreszer, E.R. Weber, Physical Review B 51 (1995) 18003.
[36] J.H. Werner, Applied Physics Letters 54 (1989) 1526.
[37] J.H. Werner, H.H. Güttler, Journal of Applied Physics 73 (1993) 1315.
[38] A. Türüt, M. Sağlam, Physica B 179 (1992) 285.
[39] J.C. Card, E.H. Rhoderick, Journal of Physics D 4 (1971) 1589.
[40] P. Cova, A. Singh, Solid State Electronics 33 (1990) 11.
[41] A. Türüt, M. Sağlam, H. Efeoğlu, N. Yalçın, M. Yıldırım, B. Abay, Physica B 205 (1995) 41.
[42] A.F. Ozdemir, D.A. Aldemir, A. Kokce, S. Altindal, Synthetic Metals 159 (2009) 1427–1432.
[43] S. Aydogan, M. Sağlam, A. Türüt, Y. Onganer, Materials Science and Engineering C 29 (2009) 1486–1490.
[44] M. Sağlam, D. Korucu, A. Türüt, Polymer 45 (2004) 7335–7340.
[45] S.K. Cheung, N.W. Cheung, Applied Physics Letters 49 (1986) 85.
[46] M. Siad, A. Keffous, S. Mamma, Y. Belkacem, H. Menari, Applied Surface Science 236 (2004) 366–376.
[47] Yasuo Koide, H. Ishikawa, S. Kobayashi, S. Yamasaki, S. Nagai, J. Umezaki, et al., Applied Surface Science 117–118 (1997) 373–379.
[48] A. Singh, Solid State Electronics 28 (1985) 223.
[49] S. Altındal, I. Dokme, M.M. Bülbül, N. Yalcin, T. Serin, Microelectronic Engineering 83 (2006) 499–505.
[50] E. Ayyildiz, B. Bati, C. Temirci, A. Türüt, Applied Surface Science 152 (1999) 57–62.
[51] S. Karatas, M. Cakar, Synthetic Metals 159 (2009) 347–351.
[52] M. Sağlam, A. Türüt, Journal of Applied Polymer Science 101 (2006) 2313–2319.
[53] S. Karatas, A. Türüt, S. Altındal, Nuclear Instruments and Methods in Physics Research A 555 (2005) 260–265.